

DETC2014-35484

## A TECHNIQUE TO DETECT FATIGUE IN THE LOWER LIMBS

**Abdullatif A. Alwasel\***

Systems Design Engineering  
University of Waterloo  
Waterloo, Ontario, N2L 3G1  
Canada

Email: aalwasel@uwaterloo.ca

**Eihab M. Abdel-Rahman**

Systems Design Engineering  
University of Waterloo  
Waterloo, Ontario, N2L 3G1  
Canada

Email: eihab@uwaterloo.ca

**Carl T. Haas**

Civil and Environmental Engineering  
University of Waterloo  
Waterloo, Ontario, N2L 3G1  
Canada

Email: chaas@uwaterloo.ca

### ABSTRACT

*As muscles fatigue, their passive and active mechanical properties change increasing the susceptibility of the human body to damage. The state-of-the-art technique for muscle fatigue detection, EMG signals, is cumbersome. This paper presents a technique to detect fatigue by tracking a kinematic parameter of the musculoskeletal system. The method uses the time-history of a single joint angle to detect fatigue in the lower limbs. A sensor is mounted to the knee joint to measure the knee flexion angle. Time delay embedding is used to track the orbit of knee joint motions in a reconstructed phase-space. The reconstructed phase-space allows us to obtain information about other body parts and joints of the lower limb in addition to the knee joint, since they are all connected in an open kinematic chain. Long-time drift in the orbit location and shape in phase-space is quantified and used as a measure of lower limb fatigue. The proposed technique presents a mobile, wireless, and cheap method to assess fatigue that can act as an early warning system for the lower limb.*

**Keywords:** Phase space warping, Delay time embedding, Fatigue, Lower limb

### INTRODUCTION

Fatigue in human bodies is a natural process that result from the prolonged use of muscles under their threshold limits or the use of extensive muscle force for short periods of time. Unlike

many mechanical systems, fatigue process in the human body can result from the application of low magnitude of constant force for prolonged periods of time or can result from the application of cyclic loads with frequency time below the rest time allowance provided by [1, 2]. As muscles fatigue, their passive and active mechanical properties change increasing the susceptibility of the human body to damage. Detecting fatigue can help to protect against potential injury.

The state-of-the-art technique in muscle fatigue detection is through the use of EMG signals obtained by placing electrodes on the skin. EMG detects the level of action potential in the muscles. The analysis of EMG reveals if the muscle started to fatigue by observing its state and comparing it to its state when it was healthy. Acquiring EMG signals limits human motion and results in altered motion patterns due to electrode entanglement. EMG signals are weak in amplitude; thus, an amplifier is connected to the input signal before interfacing it to the computer, which introduces a white noise to the collected EMG signal. After this, the analysis work begins. Furthermore, Hardware used in collecting EMG signals also has its drawbacks because, due to the fact the human is wired to the station to collect the EMG, the human subjects tend to change the way they perform the task, which introduces noise to the signal. More important is that the EMG signal is collected inside labs. This prohibits the use of EMG to track the fatigue process among workers in real-life situations e.g. workers in production lines or in construction field. Furthermore, the use of these electrodes requires a laboratory environment.

In North America, the largest number of injuries among

---

\*corresponding author.

workers is Musculoskeletal Disorders (MSDs) [3, 4]. There are four main risk factors for MSD: forceful work, repetitive work, work above head level, and tools vibration [5]. All these risk factors have muscles fatigue in common. In other words, the prolonged exposure to these risk factors what makes the injury [6]. Through the prolonged exposure to these risk factors, the muscle dynamics change in an attempt to cope with the level of demand. This adaptation is through changing the synergy of muscles activated to perform certain motion or the alternative firing of muscle fiber, which can be observed as the human muscle starts shaking when performing a task for prolonged time. The change in synergy and muscle firing scheme is to comprise the fatigue happening to the muscle.

Muscle fatigue detection outside the lab setting can decrease the number of injuries. Through the detection of fatigue, many decisions can be made to avoid the MSD by changing the task that a worker is performing or introducing rest-time allowance for the muscles to regain its original shape and condition before the injury happen. However, there is no method to date that can measure the level of fatigue outside the lab environment.

The principles of damage tracking in dynamical systems can be used to track the slow dynamic process of muscle fatigue hidden in the kinematics of the human musculoskeletal system. Sanjari et al. [7] used the method of phase space warping (PSW) to detect fatigue in the upper limb using information embedded in the time-history of the elbow flexion angle. They collected the kinematic angle data using electrogoniometer at 50 Hz sampling rate.

This paper presents a technique to detect fatigue through the use of time delay embedding and PSW. The method uses kinematic information obtained from a single joint. In the presented work, It allows for free mobility outside a lab environment. The use of time delay embedding allows us to track the orbit of the knee joint flexion angle in the reconstructed phase-space. Long-time drift in the orbit location and shape represent the state of the knee health (fatigue). This technique will allow for mobile, wireless, and cheap sensing fatigue and provide an early warning system for potential damage to the lower limb.

## METHODOLOGY

The fatigue detection method proposed here requires data collection for a single kinematic state from a single joint in the lower limb kinematic chain. Any kinematic measurement system can be used for data collection. In this implementation, a direct measurement system [8], Fig. 1, was used to track the knee flexion angle. The system utilizes an optical encoder mounted non-invasively to an exoskeleton and placed along the joint rotation axis. The exoskeleton has two arms: one aligned with the thigh and another aligned with the shank. It saves collected data to an on-board SD card.

A healthy male right hand dominant volunteer was instru-



**FIGURE 1:** Data collection system.

mented with a direct measurement system to measure the left knee flexion angle. The subject was directed to wear the system and walk on a treadmill. He was asked to stand on the treadmill while at rest, then data collection was commenced. The treadmill speed was increased from 0 to 4.5 km/h within 10 s and maintained at that speed throughout data collection. The subject was directed to walk on the treadmill until he experiences a fatigue level that prevents him from keeping up with the treadmill. The treadmill was then brought to rest and data collection was terminated.

The collected knee flexion data was processed using time delay embedding [9] and PSW [10, 11] techniques to track fatigue in the left lower limb. Time delay embedding is used to reconstruct the phase-space of a coupled dynamic system using the time-history of a single system state  $y(t)$ . It can reveal information about the minimum dimension  $d_o$  required to represent the coupled dynamic system under consideration; the open kinematic chain of the lower limb in this case. The technique determines the proper time delay  $\tau$  of  $y$  necessary to reconstruct

phase-space, represent the missing states, and the overall number of states  $d_o$ , system dimension, embedded in the signal.

We used the fill factor algorithm [9] to determine the proper time delay and minimum dimension of the dynamic system simultaneously. The algorithm defines the function

$$F(\tau) = \frac{\sum_{i=1}^{N_s} |Det[M_d]|}{N_s(y_{max} - y_{min})^d} \quad (1)$$

where  $Det[M_d]$  is a measure of the hyper-area occupied by the orbit in phase-space of dimension  $d$ ,  $N_s$  is the number of random evaluations of the hyper-area, and  $y_{max}$  and  $y_{min}$  are the largest and smallest angles, respectively, recorded in the time series. It calculates  $F(\tau)$  as a measure of the area occupied by orbits in the reconstructed phase-space of dimension  $d$  as a function of the delay time  $\tau$ . This process is repeated as the dimension of the reconstructed state vector  $d$  is increased.

The minimum system dimension  $d_o$  is determined as the dimension beyond which the features in the  $F(\tau)$  curve do not change. That is,  $d_o$  is taken as the dimension beyond which the curve  $F(\tau)$  does not add additional minima or maxima as  $d$  increases. Therefore, curves obtained for dimensions higher than  $d_o$  are essentially parallel to each other.

As a result, the system state vector is reconstructed as

$$\mathbf{y}(t) = \left\{ \begin{array}{c} y(t) \\ y(t + \tau) \\ \vdots \\ y(t + \tau(d-1)) \end{array} \right\} \quad (2)$$

In this analysis, PSW calls for a distinction between three time-scales:

1. a fast-time scale of the same order as the sampling period  $T_s$ .
2. an intermediate time-scale of the same-order as the average gait cycle period  $T_g$ .
3. a slow time-scale where muscle fatigue can be observed.

To reduce signal noise at the fast and intermediate time-scales, the reconstructed phase-space is divided into two subsets: a reference subset made of the initial  $M_1$  gait cycles and snap shots each of size  $M_2$  gait cycles in the subsequent time-history. The times required to take the samples  $M_1$  and  $M_2$  are of the same order as  $T_g$ .

At each point  $y_n$  in the reference subset, the nearest  $N$  points are used to construct a linear map representing a linearization of the return map at that location in the reconstructed phase-space [10]:

$$\mathbf{y}_{n+1} = P(\mathbf{y}_n) \quad (3)$$

The reference subset is chosen to encompass a long-time record representing multiple gait cycles. As a result, each local return map represents averaging of the dynamics of the rested limb over the inter-mediate time-scale.

The local return maps represent the rested state of the lower limb before fatigue onset. As muscles fatigue, the measured state vector represents the return map

$$\mathbf{y}_{n+1} = \hat{P}(\mathbf{y}_n, \phi) \quad (4)$$

where  $\phi$  is a parameter representing the fatigue of the muscles. Therefore, fatigue can be estimated as the difference between the rested return map prediction of the  $k^{\text{th}}$  return and the fatigued return map:

$$e_{n+k} = \|\hat{P}(\mathbf{y}_{n+k-1}, \phi) - P^k(\mathbf{y}_n)\| \quad (5)$$

Alternatively, the fatigue tracking metric  $e_n$  can be calculated by comparing the  $k^{\text{th}}$  return predicted by the rested return map to the reconstructed state vector at that point in time:

$$e_{n+k} = \|\mathbf{y}_{n+k} - P^k(\mathbf{y}_n)\| \quad (6)$$

The fatigue metric is averaged out over each gait cycle period  $T_g$  to reduce fast and intermediate time-scales noise. Therefore, the fatigue metric is written as:

$$E_M = \frac{1}{M_2} \sum_{i=0}^{M_2} e_i \quad (7)$$

where  $M$  is the number of data points per gait cycle  $T_g$ .

## RESULTS

The data collection session lasted for four minutes until the participant could no longer keep up with the treadmill. The knee flexion angle was sampled at the rate of 500 Hz ( $T_s = 2$  ms), which is one order-of-magnitude higher than the standard rate for comparable biomechanical data. The average gait cycle was found to be  $T_g \approx 1.2$  s.

The time delay  $\tau_o$  and minimum system dimension  $d_o$  were determined using the fill factor algorithm 1. Towards that end, the fill factor function  $F(\tau)$  was evaluated, Fig. 2, for state vector dimension in the range of  $d = 2-10$  and time delays in the range of  $\tau = 1-300T_s$  incremented in steps of  $24T_s$ . Inspecting the Figure, we observe that no new minima or maxima are added beyond  $d_o = 5$ , which indicates that the minimum dimension required to represent the coupled dynamic system of the lower limb is five.

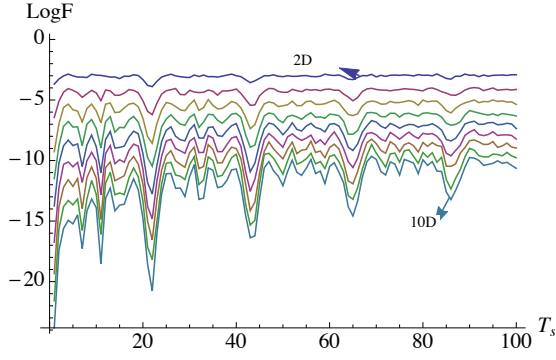


**FIGURE 2:** Log of the fill factor  $F(\tau)$  as a function of the time delay for stat vector dimensions in the range of  $d=2-10$ .

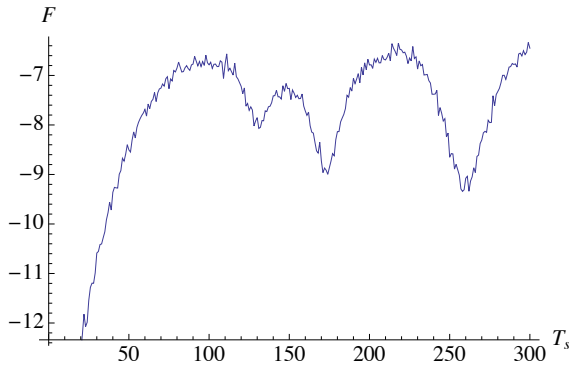


**FIGURE 3:** The fill factor of the reconstructed phase-space ( $d_o = 5$ ) as a function of time delay.

The second step in reconstructing phase-space is to determine a proper time delay that reflects the essential features of the dynamic system. Thus, we closely inspected the fill factor function  $F(\tau)$  as the time delay is increased in steps of  $1T_s$ , Fig. 3, for the first curve maxima. The proper time delay was found to be  $\tau_o = 100T_s$ .

We used  $d_o$  and  $\tau_o$  to reconstruct the pseudo phase-portrait of the knee flexion angle shown in Figure 4. For comparison, we present in Figure 5 the phase-portrait of the knee flexion angle obtained from the measured kinematic data of the gait cycle [12]. The two figures are in qualitative agreement establishing the dynamic equivalence of the two orbits. Specifically, both phase-portraits show two loops; a large loop representing the leg swing phase and a small loop representing the heel strike-toe off phase of the human gait cycle.

The local linear map is composed of a parameter matrix  $\mathbf{A}_n$  and a parameter vector  $\mathbf{a}_n$  that describe the  $k^{\text{th}}$  return of the state

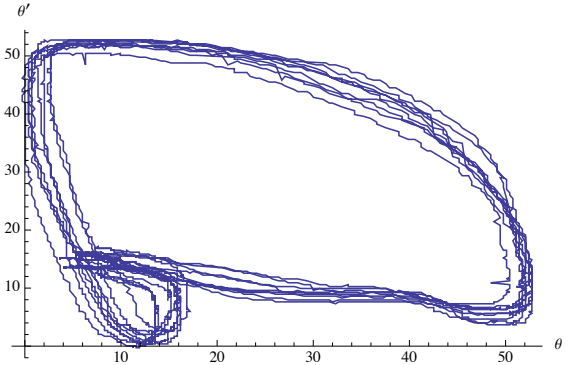


**FIGURE 4:** The pseudo phase-portrait of the knee angle obtained from delay embedding.

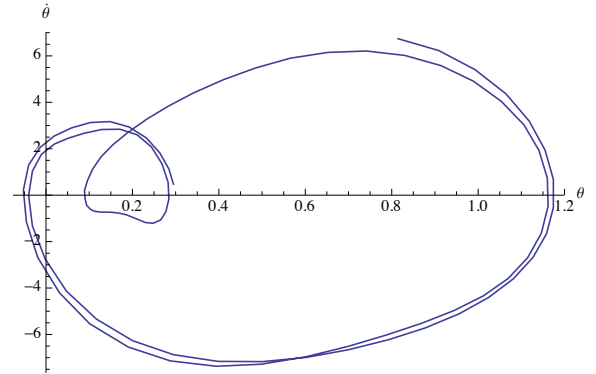


**FIGURE 5:** The phase-portrait of the knee angle extracted from [12].

vector  $\mathbf{y}_n$  according to:

$$\mathbf{y}_{(n+k)} = \mathbf{A}_n \mathbf{y}_n + \mathbf{a}_n \quad (8)$$

The map parameters  $\mathbf{A}_n$  and  $\mathbf{a}_n$ , are calculated following the procedure described in [10] from a matrix

$$\mathbf{Y}_n = [\mathbf{y}_n^1 \ \mathbf{y}_n^2 \ \dots \ \mathbf{y}_n^N] \quad (9)$$

constructed out of the  $N = 15$  nearest neighbors of  $\mathbf{y}_n$  in the reference set.

The reference times series was made of the initial  $M_1 = 10$  gait cycles and each of the snap shots were taken to be  $M_2 = 10$  gait cycles. The tracking function  $e_n$  was calculated for each gait cycle  $T_g$  in the reference and tracking snap shots. The results are shown in Fig 6. The numerical values on the y-axis represent the average change in the reconstructed phase-space of each

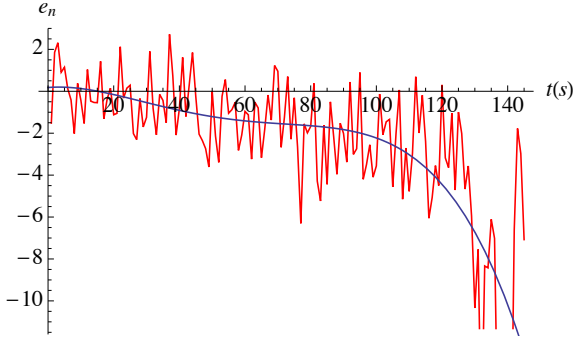


**FIGURE 6:** Tracking metric  $e_n$  as a function of time.

gait cycle. The average gait cycle was estimated from the reference times series representing the healthy state of lower limb. Superimposed on the figure is a quadratic fit of the tracking metric  $e_n$  as a function of time representing the slow-time trend of the lower limb health (fatigue state). As shown in Fig. 6, fatigue starts to appear after 15 s and increases monotonically reaching a maximum as the subject fails to keep up with the treadmill.

## DISCUSSION

The system examined in this work is the open kinematic chain of the lower limb that starts from the trunk and ends at the foot. The measured state is the knee flexion angle  $\theta$  representing partial information on a part of the kinematic chain. The flexion angle was obtained using a direct measurement system [8] that provides drift-free angle measurements, unlike other systems used to measure kinematic parameters outside a laboratory environment which suffer from long-time drift.

The time-history of the measured flexion angle carries information about the other states of the coupled dynamic system of the lower limb. Using time delay embedding, we determined that the minimum system dimension was  $d_o = 5$  and reconstructed the pseudo phase-space.

We hypothesis that those states correspond to a two-rigid bodies dynamic model of the lower limb in the sagittal plane, namely the shank and thigh connected by a hinge joint. This model consists of four independent states, representing knee and thigh flexion angles  $\theta$  and  $\alpha$  and their angular speeds  $\dot{\theta}$  and  $\dot{\alpha}$ , and a fifth state representing the forcing phase angle  $\beta(t)$  imposed on the system by the treadmill. Thus, the state vector of the dynamic system can be written as  $y(t) = [\theta, \dot{\theta}, \alpha, \dot{\alpha}, \beta]$ .

The pseudo phase-space is, therefore, reconstructed to represent the discrete time evolution of the state vector  $\mathbf{Y}_n = [\theta, \dot{\theta}, \alpha, \dot{\alpha}, \beta]$ . Orbits of knee flexion obtained in the pseudo phase-space show qualitative agreement with those measured by Winter [13]. However, the orbits obtained here show significant ‘noise’ cycle-on-cycle orbit variability.

There are various possible sources for this noise observed in the response of the lower limb. Previous tests have shown that the accuracy of the direct angle measurement system is better than  $0.3^\circ$  [8] indicating that the contribution of measurement noise to the overall signal noise is relatively low. An important source of ‘noise’ is the neural input of the central nervous system (CNS) to the gait cycle. As shown by Winter [13], human gait approximates an inverted pendulum whose mass is located at the center of body mass, located anterior to the foot center of pressure throughout the gait cycle, which requires continuous feedback by the CNS to stabilize posture. This effect can be observed as cycle-on-cycle variation in the gait cycle dynamics. It represents fast intra-cycle signal variations of the same order as the sampling period  $T_s$ .

A local linear map constructed at time  $n$ , when the muscles are in their baseline healthy state, allows us to track the slow-time changes occurring due to muscles fatigue by comparing map prediction of the state vector at time  $n + k$  to the actual, fatigued, state vector at the same point in time. PSW estimates the difference between the predicted and measured state vector and average it out per gait cycle to obtain a damage metric  $e_n$ . The time history of this metric  $e_n$ , Fig6, represents the damage (muscle fatigue) evolution over slow time.

Therefore, the combination of delay time embedding and PSW provides a ‘big picture’ estimator of fatigue in the lower limb using the time-history of a single joint angle. Unlike state-of-the-art fatigue detection techniques [14], this method can supply information about fatigue evolution outside a laboratory environment. This opens doors to applications such as tracking the physical state of players in a field, workers in a plant, and patients undergoing in-home rehabilitation.

## CONCLUSION

This paper presented a technique to track fatigue evolution in the lower extremities. The technique uses delay time embedding to reconstruct phase space from a measurement of a single joint state, knee flexion angle in this case. It then uses the method of phase space warping to track the slow time changes in muscle health state (fatigue). Flexion angle data is collected using a drift-free joint angle measurement system.

Our results show that this technique can be readily deployed to monitor players in a field or patients during in-home rehabilitation. Using this technique can provide a feedback system to players, patients, workers, and health care professionals that can be used to decrease injuries due to fatigue.

## ACKNOWLEDGMENT

The first author would like to acknowledge King Saud University support of his PhD program.

## REFERENCES

- [1] W. Rohmert, "Determination of Relaxation Periods in Industrial Operations, Part 1," *Work Study and Management*, vol. 8, no. 11, pp. 500–505, 1964.
- [2] W. Rohmert, "Determination of Relaxation Periods in Industrial Operations, Part 2," *Work Study and Management*, vol. 8, no. 11, pp. 550 – 556, 1964.
- [3] Bureau of Labor Statistics U S Department of Labor, "Nonfatal occupational injuries and illnesses requiring days away from work, 2011," Tech. Rep. 202, U.S. Department of labor, 2012.
- [4] Statistics Canada, "Work absence rates," 2011.
- [5] B. P. Bernard, *Musculoskeletal Disorders and Workplace Factors. A Critical Review of Epidemiologic Evidence for Work-Related Musculoskeletal Disorders of the Neck, Upper Extremity, and Low Back*. Cincinnati, OH.: National Institute for Occupational Safety and Health (NIOSH), 1997.
- [6] S. Kumar, "Theories of Musculoskeletal Injury Causation," *Ergonomics*, vol. 44, pp. 17–47, Jan. 2001.
- [7] M. A. Sanjari, A. R. Arshi, M. Parnianpour, and S. Seyed-Mohseni, "Local State Space Temporal Fluctuations: A Methodology to Reveal Changes During a Fatiguing Repetitive Task.," *Journal of biomechanical engineering*, vol. 132, p. 101002, Oct. 2010.
- [8] A. Alwasel, K. Elrayes, E. Abdel-Rahman, and C. Haas, "A Human Body Posture Sensor for Monitoring and Diagnosing MSD Risk Factors," in *The 30th International Symposium on Automation and Robotics in Construction, Montreal, Canada*, 2013.
- [9] T. Buzug and G. Pfister, "Optimal Delay Time and Embedding Dimension for Delay-time Coordinates by Analysis of the Global Static and Local Dynamical Behavior of Strange Attractors," *Physical review A*, vol. 45, no. 10, pp. 7073–7084, 1992.
- [10] D. Chelidze, J. P. Cusumano, and A. Chatterjee, "A Dynamical Systems Approach to Damage Evolution Tracking, Part 1: Description and Experimental Application," *Journal of Vibration and Acoustics*, vol. 124, no. 2, p. 250, 2002.
- [11] J. P. Cusumano, D. Chelidze, and A. Chatterjee, "A Dynamical Systems Approach to Damage Evolution Tracking, Part 2: Model-Based Validation and Physical Interpretation," *Journal of Vibration and Acoustics*, vol. 124, no. 2, p. 258, 2002.
- [12] D. A. Winter, *Biomechanics and Motor Control of Human Movement*. Wiley, fourth ed., 2009.
- [13] D. A. Winter, "Biomechanical Movement Synergies," in *Biomechanics and Motor Control of Human Body*, ch. Biomechanical Movement Synergies, pp. 281–295, Wiley, fourth ed., 2009.
- [14] H. Dong, I. Ugalde, N. Figueroa, and A. E. Saddik, "Towards Whole Body Fatigue Assessment of Human Movement: A Fatigue-Tracking System Based on Combined sEMG and Accelerometer Signals," *Sensors*, vol. 14, pp. 2052–70, Jan. 2014.